Available online at www.sciencedirect.com
ScienceDirect
J. Vis. Commun. Image R. 18 (2007) 406–414
JOURNAL OF VISUAL Communication & IMAGE Representation
www.elsevier.com/locate/jvci

iCAM06: A refined image appearance model for HDR image rendering

Jiangtao Kuang *, Garrett M. Johnson, Mark D. Fairchild

Munsell Color Science Laboratory, Rochester Institute of Technology, 54 Lomb Memorial Dr., Rochester, NY 14623, USA

Received 15 November 2006; accepted 12 June 2007
Available online 27 June 2007

Abstract

A new image appearance model, designated iCAM06, was developed for High-Dynamic-Range (HDR) image rendering. The model, based on the iCAM framework, incorporates the spatial processing models in the human visual system for contrast enhancement, photoreceptor light adaptation functions that enhance local details in highlights and shadows, and functions that predict a wide range of color appearance phenomena. Evaluation of the model proved iCAM06 to have consistently good HDR rendering performance in both preference and accuracy making iCAM06 a good candidate for a general-purpose tone-mapping operator with further potential applications to a wide-range of image appearance research and practice.

Keywords: Image appearance; HDR imaging; Tone mapping; Rendering; Vision modeling; Tone-mapping operator testing

1. Introduction

Color appearance models have been applied in cross-media color reproduction frameworks; however, they are limited in scope and are not designed for prediction of visual appearance of complex spatially varying stimuli such as images or videos. Image appearance models extend color appearance models to incorporate properties of spatial and temporal vision allowing prediction of the appearance of complex stimuli. Given an input of images and viewing conditions, an image appearance model can provide perceptual attributes of each pixel, not only limited to the traditional color appearance correlates such as lightness, chroma and hue, but rather those image attributes such as contrast and sharpness. The inverse model can also take the output viewing conditions into account and thus generate the desired output perceptual effect for color image reproduction.

Spatial color appearance models, e.g., S-CIELAB [1], were first proposed by incorporating spatial filtering to measure the difference between two images, extending the application of traditional color difference equations in measuring the perceptual difference between complex stimuli. The filtering computation is dependent on viewing distance and is generally derived from human contrast sensitivity functions. For spatial vision and color appearance prediction, the spatial filtering is sometimes broken down into multiple channels for various spatial frequencies and orientations, for example, the Multi-scale Observer Model (MOM) [2]. More recent results suggest that while such multi-scale filtering might be critical for some threshold metrics, it is often not necessary for supra-threshold predictions of image attributes and perceived image differences. Image color appearance model (iCAM) [3–5] was thus proposed to preserve simplicity and ease of use by adopting a single-scale spatial filtering.

High dynamic range (HDR) imaging has been an active research area in the last two decades. In real-world scenarios one might encounter a wide range of luminance (up to 9 log units) between the highlights and the shadows. Imaging technology has advanced such that the capture and storage of this broad dynamic range is now possible, but the output limitations of common desktop displays as well as hard-copy prints have not followed the same advances. HDR rendering algorithms, which are also known as tone-mapping operators (TMOs), are designed to scale the large

* Corresponding author.
E-mail address: jxk4031@cis.rit.edu (J. Kuang).

1047-3203/$ - see front matter © 2007 Elsevier Inc. All rights reserved.
doi:10.1016/j.jvcir.2007.06.003

range of luminance information that exists in the real world so that it can be displayed on a device that is only capable of producing a much lower dynamic range. The goals of these algorithms vary considerably dependent on their specific applications. For instance, algorithms are designed to provide the maximum amount of detail information in medical imaging, as might be desirable for a radiologist examining medical MR images. In digital photography, goals might include, but of course are not limited to, producing pleasing or preferred pictorial images, reproducing overall appearance between the original and display, maintaining contrast relationships between objects in the scene, maintaining the original photographers' intent, and predicting visibility of specific objects in a scene. As image appearance models attempt to predict the perceptual response towards spatial complex stimuli, they can provide a unique framework for the prediction of the appearance of HDR images. Without changing its general framework, iCAM has been extended into the application of HDR image rendering [6].

Recent tone-mapping operator evaluation results [7] showed that iCAM is effective in HDR image rendering; however, iCAM does not perform as well as some of other operators, such as the bilateral filter [8], which incorporate efficient anisotropic filters but simple tone compression strategies. Even for the reproduction accuracy evaluation, where iCAM is most applicable, the renderings of iCAM were found to contain less local contrast and colorfulness compared with original scenes. This motivates further improvements of iCAM for the application of HDR image rendering by incorporating properties of previous tone-mapping operators.

The next generation of image appearance model, designated iCAM06, was developed for HDR image rendering application [9–11]. Several modules have been inherited from the iCAM framework, such as the local white point adaptation, chromatic adaptation, and the IPT uniform color space. A number of improvements have been implemented in iCAM06 on the motivation of a better algorithm that is capable of providing more pleasing and more accurate HDR renderings, and even a more developed perceptual model for a wider range of image appearance prediction. The modifications considered and ultimately incorporated in iCAM06 in some form included:

- Replaced the single-scale Gaussian filtering in iCAM with a two-layer image decomposition using an edge-preserving bilateral filter and dual image processing framework;
- Replaced the simple non-linear local gamma correction in iCAM with the photoreceptor response functions from previous color appearance research;
- Extended, through incorporation of scotopic and photopic signals, to a large range of luminance levels;
- Incorporated a luminance dependent local contrast enhancement module, which simulates the contrast changes suggested by the Stevens effect;
- Incorporated a luminance dependent local colorfulness enhancement module, which simulates the colorfulness changes predicted by the Hunt effect;
- Incorporated a surround luminance dependent correction module, which accounts for the perceptual gamma changes predicted by the Bartleson–Breneman surround effect.

After the present section, which serves as an introduction to this research, Section 2 describes the implementation of the iCAM06 model for the application of HDR image rendering. The testing results of iCAM06 comparing to previous tone-mapping operators are presented in Section 3, followed by concluding remarks in Section 4.

2. Framework of the iCAM06 model

The goal of the iCAM06 model is to accurately predict human visual attributes of complex images in a large range of luminance levels and thus reproduce the same visual perception across media. The general flowchart of iCAM06 for HDR image rendering is shown in Fig. 1. Note that although the iCAM06 framework described in this section focuses on HDR image rendering, the parameters or modules can be specifically tuned for a wide range of situations, including, but not limited to, spatial vision phenomena prediction [11] and image difference calculation.

2.1. Input data

The input data for iCAM06 model are CIE tristimulus values (XYZ) for the stimulus image or scene in absolute luminance units. The absolute luminance Y of the image data is necessary to predict various luminance-dependent phenomena, such as the Hunt effect and the Stevens effect. An HDR image input is typically a floating point RGB image linear to absolute luminance. Ideally, a RGB encoded image can be transformed into CIE 1931 XYZ tristimulus values through the specific camera characterization. However, the camera characteristics are generally not included in the image file. An example transformation using the sRGB color space [12] transform matrix is described in Eq. (1).

$$\begin{bmatrix} X \\ Y \\ Z \end{bmatrix} = M_{\mathrm{sRGB}} \begin{bmatrix} R \\ G \\ B \end{bmatrix}, \quad M_{\mathrm{sRGB}} = \begin{bmatrix} 0.4124 & 0.2127 & 0.0193 \\ 0.3576 & 0.7152 & 0.1192 \\ 0.1805 & 0.0722 & 0.9504 \end{bmatrix} \tag{1}$$

2.2. Image decomposition

Once the input image is in device independent coordinates, the image is decomposed into a base layer, containing only large-scale variations, and a detail layer. The modules of chromatic adaptation and tone-compression processing are only applied to the base layer, thus

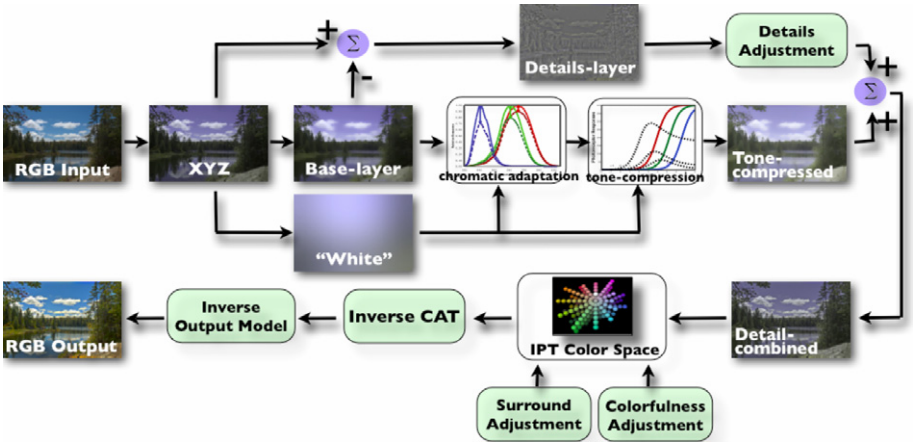

Fig. 1. Flowchart of iCAM06.

preserving details in the image. The two-scale decomposition is motivated by two widely accepted assumptions in human vision: (1) An image is regarded as a product of the reflectance and the illumination, and human vision is mostly sensitive to the reflectance rather than the illumination conditions; (2) human vision responses mostly to local contrast instead of the global contrast. These two assumptions are actually closely related since the local contrast is accordance to the reflectance in an image in some way. The fact that the human visual system is insensitive to the global luminance contrast enables the solution of compressing the global dynamic range and preserving local details in an HDR scene to reproduce the same perceptual appearance on a LDR display that has a significantly lower maximum absolute luminance output.

The base layer is obtained using an edge-preserving filter called bilateral filter, previously proposed by Durand and Dorsey [8]. Bilateral filter is a non-linear filter, where each pixel is weighted by the product of a Gaussian filtering in the spatial domain and another Gaussian filtering in the intensity domain that decreases the weight of pixels with large intensity differences. Therefore, bilateral filter effectively blurs an image while keeps sharp edges intact, and thus avoids the "halo" artifacts that are common for local tone-mapping operators. The pixel intensity calculations are performed in the log domain because the pixel differences are directly corresponding to the perceptual contrast, and also because it yields a more uniform treatment of the whole image. The output of the bilateral filter for a pixel s is expressed in Eqs. (2) and (3):

$$J_s = \frac{1}{k(s)} \sum_{p \in \Omega} f(p-s) g(I_p - I_s) I_p \tag{2}$$

where $k(s)$ is a normalization term:

$$k(s) = \sum_{p \in \Omega} f(p-s) g(I_p - I_s) \tag{3}$$

$f(\ )$ is a Gaussian function in the spatial domain with the kernel scale σ_s set to empirical value of 2% of the image size, and $g(\ )$ is another Gaussian function in the intensity domain with its scale σ_r set to a constant value of 0.35 [8]. I_s is the intensity value for pixel s, which is influenced mainly by pixels that are close spatially and that have a similar intensity. The bilateral filtering is speeded up using a piecewise-linear approximation and nearest neighbor down sampling [8] in iCAM06.

The detail layer is then achieved by subtracting the base layer image from the original image. Both of the two layers are then transformed back into the linear domain for the following processing.

2.3. Chromatic adaptation

The base layer image is first processed through the chromatic adaptation. The chromatic adaptation transformation embedded in iCAM, which is originally from CIECAM02 [13], has been adopted in the iCAM06 model. It is a linear von Kries normalization of the spectral sharpened RGB image signals by the RGB adaptation white image signals derived from the Gaussian low-pass adaptation image at each pixel location ($R_w G_w B_w$). The amount of blurring in the low-pass image is controlled by the half-width of the filter σ, which is suggested to set to 5-degree radius of background [14]. The characteristics of the viewing conditions are often unknown for HDR image rendering application; thus a simplifying assumption can be to specify the width of the filter according to the image size itself. One half of the smaller dimension size of the image performed consistently well for our experiments and is used in the iCAM06 implementation. The computations of the transform are given in Eqs. (4)–(8).

$$\begin{bmatrix} R \\ G \\ B \end{bmatrix} = M_{CAT02} \begin{bmatrix} X \\ Y \\ Z \end{bmatrix}, M_{CAT02} = \begin{bmatrix} 0.7328 & 0.4296 & -0.1624 \\ -0.7036 & 1.6975 & 0.0061 \\ 0.0030 & 0.0136 & 0.9834 \end{bmatrix} \tag{4}$$

$$D = 0.3F\left[1 - \left(\frac{1}{3.6}\right) e^{\left(\frac{-(L_A-42)}{92}\right)}\right] \tag{5}$$

$$R_c = \left[\left(R_{D65}\frac{D}{R_W}\right) + (1-D)\right] R \tag{6}$$

$$G_c = \left[\left(G_{D65}\frac{D}{G_W}\right) + (1-D)\right]G \tag{7}$$

$$B_c = \left[\left(B_{D65}\frac{D}{B_W}\right) + (1-D)\right]B \tag{8}$$

The transform begins with a conversion from CIE XYZ image to the spectrally sharpened RGB image using the transformation matrix M_{CAT02} in the formulation of CIECAM02 [13]. The incomplete adaptation factor D is computed as a function of adaptation luminance L_A (20% of the adaptation white) and surround factor F ($F = 1$ in an average surround). In theory this value ranges from 0 for no adaptation to 1 for complete adaptation, and in practice the minimum value will not be less than 0.65 for a dark surround and exponentially converge to 1 with increasing values of L_A. Note that a scale factor of 0.3 is applied to the D factor calculation in iCAM06 to reduce the color de-saturation for HDR image rendering. The chromatic adaptation transform also converts the global white point to CIE illuminant D65 that are used in the IPT color space in a later stage, because IPT color space is defined in D65 [15].

2.4. Tone compression

The iCAM06 model is extended to luminance levels ranging from low scotopic to photopic bleaching levels. The post-adaptation nonlinear compression is a simulation of the photoreceptor responses, including cones and rods. Therefore, the tone compression output in iCAM06 is a combination of cone response and rod response.

The CIECAM02 post-adaptation model is adopted as cone response prediction in iCAM06 since it was well researched and established to have good prediction of all available visual data. The chromatic adapted RGB responses are first converted from the CAT02 space to Hunt-Pointer-Estevez fundamentals using the CIECAM02 formula, given in Eq. (9).

$$\begin{bmatrix} R' \\ G' \\ B' \end{bmatrix} = M_{HPE}M_{CAT02}^{-1}\begin{bmatrix} R_C \\ G_C \\ B_C \end{bmatrix},$$

$$M_{HPE} = \begin{bmatrix} 0.38971 & 0.68898 & -0.07868 \\ -0.22981 & 1.18340 & 0.04641 \\ 0.0 & 0.0 & 1.0 \end{bmatrix} \tag{9}$$

$$M_{CAT02}^{-1} = \begin{bmatrix} 1.096124 & -0.278869 & 0.182745 \\ 0.454369 & 0.473533 & 0.072098 \\ -0.009628 & -0.005698 & 1.015326 \end{bmatrix}$$

The nonlinear tone compression functions, shown in Eq. (10)–(14), are similar in form to those in CIECAM02, but slightly modified the power value to a user-controllable variable p, which accounts for the steepness of the response curves in Fig. 2. The value p can be set in a range of 0.6–0.85, where the larger value generates higher overall contrast in the rendered image output. A default value is empirically set to 0.75 from a pilot parameter setting experiment. This function is based on a generalized Michaelis–Menten Equation [16] and is consistent with Valeton and van Norren's experimental data [17]. The specifics and advantages of this equation were discussed by Hunt [18].

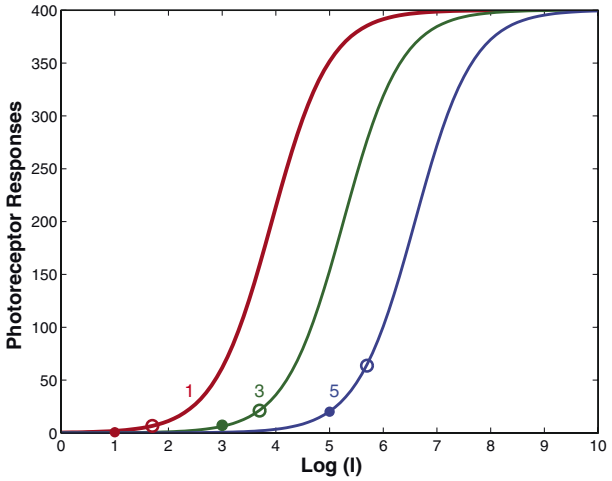

Fig. 2. Cone response after adaptation plotted against log intensity (log cd/m^2) for three adaptation levels in iCAM06. Open circles: reference whites; filled circles: adapting luminances.

$$R'_a = \frac{400(F_L R'/Y_W)^p}{27.13 + (F_L R'/Y_W)^p} + 0.1 \tag{10}$$

$$G'_a = \frac{400(F_L G'/Y_W)^p}{27.13 + (F_L G'/Y_W)^p} + 0.1 \tag{11}$$

$$B'_a = \frac{400(F_L B'/Y_W)^p}{27.13 + (F_L B'/Y_W)^p} + 0.1 \tag{12}$$

$$F_L = 0.2k^4(5L_A) + 0.1(1-k^4)^2(5L_A)^{1/3} \tag{13}$$

$$k = 1/(5L_A + 1)) \tag{14}$$

The F_L function, given in Eqs. (13) and (14), is used to predict a variety of luminance-dependent appearance effects in CIECAM02 and earlier models. However, the computation of the F_L factor in iCAM06 is quite different from that in the previous color appearance models, as it is derived from the low-pass adaptation image at each pixel location and thus spatially varied in iCAM06. Y_w is the luminance of the local adapted white image. A filter size of 1/3 the shorter dimension of the image size works well for our experimental images, though again it should be stressed that this is based on an assumption for the viewing conditions. For unusually large or small images this parameter might need to be altered. More discussions about how parameters influence the rendering results can be found in the previous publication [6].

The rods' response functions are adapted from those used in the Hunt Model [19]. The nonlinear response function is taken to be the same as that for the cones in Eqs. (10)–(13). The rod response after adaptation, A_s, is given in Eqs. (15)–(19).

$$A_s = 3.05B_s\left[\frac{400(F_{LS}S/S_w)^p}{27.13+(F_{LS}S/S_w)^p}\right]+0.3 \tag{15}$$

$$F_{LS} = 3800j^2(5L_{AS}/2.26)+0.2(1-j^2)^4(5L_{AS}/2.26)^{1/6} \tag{16}$$

$$L_{AS} = 2.26L_A \tag{17}$$

$$j = 0.00001/[(5L_{AS}/2.26)+0.00001] \tag{18}$$

$$B_S = 0.5/\{1+0.3[(5L_{AS}/2.26)(S/S_w)]^{0.3}\} + 0.5/\{1+5[5L_{AS}/2.26]\} \tag{19}$$

Here, S is the luminance of each pixel in the chromatic adapted image, i.e., the Y image, and S_w is the value of S for the reference white. By setting S_w to a global scale from the maximum value of the local adapted white point image, the rod response output is automatically adjusted by the general luminance perception of the scene. For example, the rod responses for a bright scene become significantly small comparing to the cone responses in this case. L_{AS} is the scotopic luminance, B_S is the rod pigment bleach or saturation factor, and F_{LS} is the scotopic luminance level adaptation factor. The calculations of these terms (Eq. (16)–(19)) are faithful to the original Hunt model, and more specifics were reviewed by Hunt [19]. The response functions for the rods are plotted in Fig. 3.

The final tone compression response is a sum of the cone response and the rod response, given in Eq. (20).

$$RGB_{TC} = RGB'_a + A_S \tag{20}$$

2.5. IPT transformation

The next stage of the model is to convert from the tone-compressed RGB signals back to CIE XYZ image, and combine it with the detail layer image. The tone-mapped image is then converted into IPT uniform opponent color space, where I is the lightness channel, P is roughly analogous to a red-green channel, and T a blue-yellow channel.

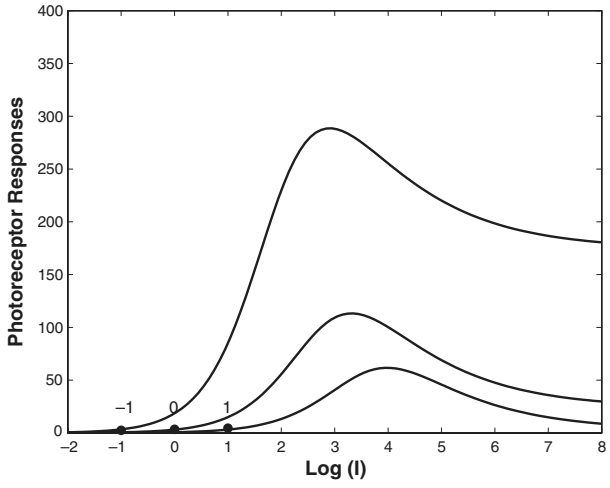

Fig. 3. Response functions for the rods in iCAM06. The rod signal, A_s, is plotted against log luminances for three adaptation levels −1, 0 and 1, respectively.

The opponent color dimensions and image attributes, such as lightness, hue, and chroma, can be derived from IPT fundamentals for image difference and image quality predictions. For HDR image rendering application, the perceptual uniformity of IPT is also necessary for the desired image attribute adjustments without affecting other attributes. The XYZ units are first converted into LMS cone responses, followed by a nonlinear power function compression, then converted into IPT units. The transformations are given in Eqs. (21)–(23) [15].

$$\begin{bmatrix}L\\M\\S\end{bmatrix} = M_H^{D65}\begin{bmatrix}X_c\\Y_c\\Z_c\end{bmatrix}, M_H^{D65} = \begin{bmatrix}0.4002 & 0.7075 & -0.0807\\ -0.2280 & 1.1500 & 0.0612\\ 0.0000 & 0.0000 & 0.9184\end{bmatrix} \tag{21}$$

$$\begin{aligned}L' &= L^{0.43}\\ M' &= M^{0.43}\\ S' &= S^{0.43}\end{aligned} \tag{22}$$

$$\begin{bmatrix}I\\P\\T\end{bmatrix} = M_{\mathrm{IPT}}\begin{bmatrix}L'\\M'\\S'\end{bmatrix}, M_{\mathrm{IPT}} = \begin{bmatrix}0.4000 & 0.4000 & 0.2000\\ 4.4550 & -4.8510 & 0.3960\\ 0.8056 & 0.3572 & -1.1628\end{bmatrix} \tag{23}$$

2.6. Image attribute adjustments

Three image attribute adjustments are implemented in iCAM06 to effectively predict image appearance effects. In the detail-layer processing, details adjustment is applied to predict the Stevens effect, i.e., an increase in luminance level results in an increase in local perceptual contrast. The detail adjustment is given in Eq. (24).

$$\mathrm{Details}_a = \mathrm{Details}^{(F_L+0.8)^{0.25}} \tag{24}$$

The power-function adjustment is luminance dependent by incorporating the F_{L} factor in the exponent. The exponent function is plotted against F_{L} in Fig. 4. The exponent monotonically increases with the F_{L} function.

In the IPT color space, P and T are enhanced to predict the Hunt effect, which predict the phenomenon that an increase in luminance level results in an increase in perceived colorfulness. The adjusted P and T are functions of the F_{L} factor and the chroma value, given in Eq. (25) and (26). The respective response function is plotted in Fig. 5. Both functions are monotonically increasing, indicating that the colorfulness of low chroma and low luminance color are more preserved than other colors. Since natural objects often have low chroma, this enhancement preserves the natural appearance of these objects.

$$P = P\cdot\left[(F_L+1)^{0.2}\left(\frac{1.29C^2-0.27C+0.42}{C^2-0.31C+0.42}\right)\right] \tag{25}$$

$$T = T\cdot\left[(F_L+1)^{0.2}\left(\frac{1.29C^2-0.27C+0.42}{C^2-0.31C+0.42}\right)\right] \tag{26}$$

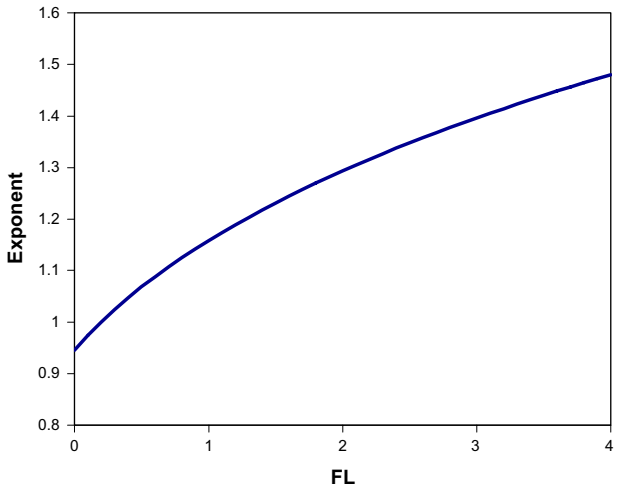

Fig. 4. Exponent function for details adjustment accounting for the Stevens effect.

The perceived image contrast increases when the image surround is changed from dark to dim to light. This effect is predicted using power functions with exponent values of 1, 1.25 and 1.5 for dark, dim and average surround, respectively [19]. To compensate these changes, a power function is applied to I channel in IPT space with exponents in the reverse order (Eq. (27)).

$$I_a = I^{\gamma}, \quad \text{where } \gamma_{\text{dark}} = 1.5, \gamma_{\text{dim}} = 1.25, \gamma_{\text{average}} = 1.0 \qquad (27)$$

2.7. Image output

To display the rendered image on an output device, the IPT image is first converted back to CIE XYZ image, followed by an inverted chromatic adaptation transform, from D65 to the output media white point using Eqs. (4)–(8) again. The inverse output characterization model then is used to transformed XYZ values to the linear device dependent RGB values using Eq. (1). An empirical clipping to the 1st and 99th percentile [6] of the image data is conducted to remove any extremely dark or bright pixels prior to display to improve the final rendering. The final images can be outputted by accounting for the device nonlinearity and scaling the images between 0 and 255.

3. Testing the iCAM06 model

3.1. Experiment overview

When a new algorithm is proposed, it is necessary to evaluate its performance comparing with other previous well-performed algorithms using a trustworthy methodology [7]. In this chapter, the iCAM06 model was tested for both perceptual accuracy of reproducing the real-world scenes and rendering preference for a large variety of HDR images.

In this experiment, four of the most successful tone-mapping operators in previous psychophysical testing experiments [7], the bilateral filter [8], photographic reproduction [20], iCAM [6], and histogram equalization [21], and two Photoshop™ CS2 HDR conversion methods, Exposure and Gamma, and Local Adaptation, together with iCAM06, are evaluated by twenty-three observers with normal color vision. By incorporating the Photoshop tools in this evaluation, the performance of the new algorithm can be compared with that of commercial software, which is more familiar to the general researchers. As those tools need manual tuning of a number of free parameters, the rendering images output are the best results carefully adjusted in Photoshop CS2 under the same experimental conditions by the author based on the image preference. Details of the experimental and results are discussed in the following.

3.2. Experimental design

The method of paired-comparison was used in the psychophysical experiment design. Experimental setup was the same as previous testing experiments [7]. The rendering

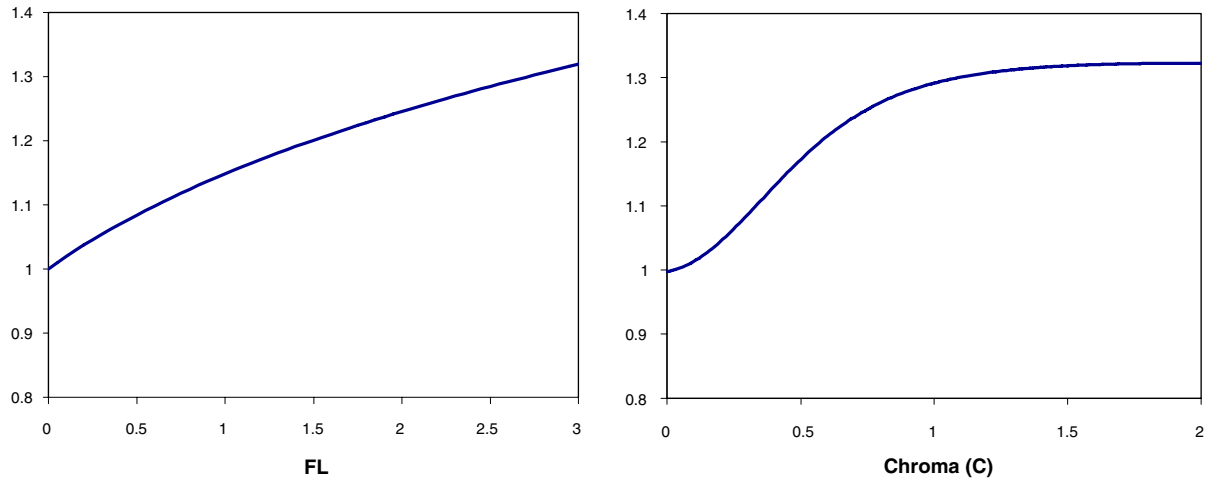

Fig. 5. Multiplication functions for colorfulness adjustment accounting for Hunt effect.

results were displayed on a colorimetric characterized 23-inch Apple Cinema HD LCD Display with the maximum luminance of 180 cd/m^2, on a gray background with a luminance of 20% of the adapting white point.

Without viewing the original scenes, observers were first presented with the task of selecting which of the two simultaneously displayed images they preferred based on the overall impression on image quality, such as contrast, colorfulness, image sharpness, and overall natural appearance, etc. A total of 252 pairs of comparison (7 algorithms for 12 test images (Fig. 6)) were included in this section, and it took about 30 min to complete.

Observers were then asked to evaluate the overall rendering accuracy comparing the overall appearance of the rendered images with their corresponding real-world scenes (the last four images in Fig. 6), which were separately set up in an adjoining room to avoid interaction. As the white points and luminance ranges of the display and the physical scenes were very different, observers were obligated to have at least 30 s of adaptation time for both the real-world scenes, and the LCD display. The observers were allowed to complete 7 pairs of comparison in one sitting based upon their memory before they were obligated to look at the original scenes again, though they could go back to view the scenes anytime they felt it necessary. By enforcing repeated viewing of the original scene it was intended to ensure that observers made their judgment based on the rendering accuracy instead of their own preference. There were a total of 84 comparisons (7 algorithms and 4 scenes) in this section, and it took approximately 20 min to complete. More details about the experimental methodologies and scenes' statistics can be found in a previous publication [7].

3.3. Results for image preference evaluation

It is observed that the rendering images of iCAM06 have more natural colors and contrast levels, and thus are more faithful to the real-world scenes and more preferable to those of other HDR rendering algorithms. The output of iCAM06 has more colorfulness and local contrast comparing to the iCAM model. The preference scores shown in Fig. 7 are the average scores of the overall paired comparison evaluations made for all test HDR images. The interval scale along with 95% confidence limits was generated using Thurston's Law of Comparative Judgments, Case V. Each algorithm is shown along the ordinate in the order of average score value. It can be seen that the new algorithms, iCAM06, performed significantly better than the other algorithms. The four previously tested tone-mapping operators have the same preference scores order as the previous results [7], but have significant lower scores than iCAM06. Two Photoshop methods locate in the middle of the preference scale, with lower preference scores than those of iCAM06 and the bilateral filter.

The results obtained for individual test images are shown in Figs. 8 and 9. The results show that iCAM06

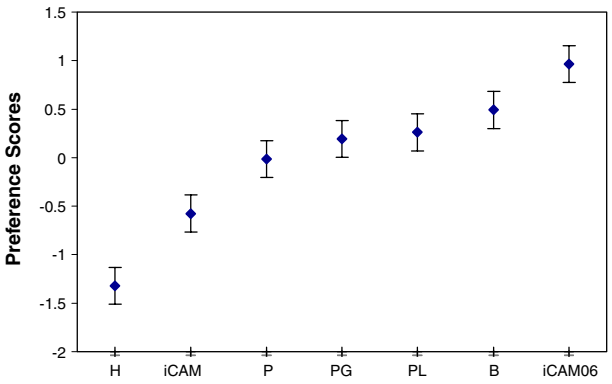

Fig. 7. Overall preference scores of tone-mapping operators over 12 HDR images (The operators are labeled as Histogram Adjustment (H), iCAM, Photographic Reproduction (P), Photoshop Exposure and Gamma (PG), Photoshop Local Adaptation (PL), Bilateral Filter (B) and iCAM06. The same labels are used in this paper.).

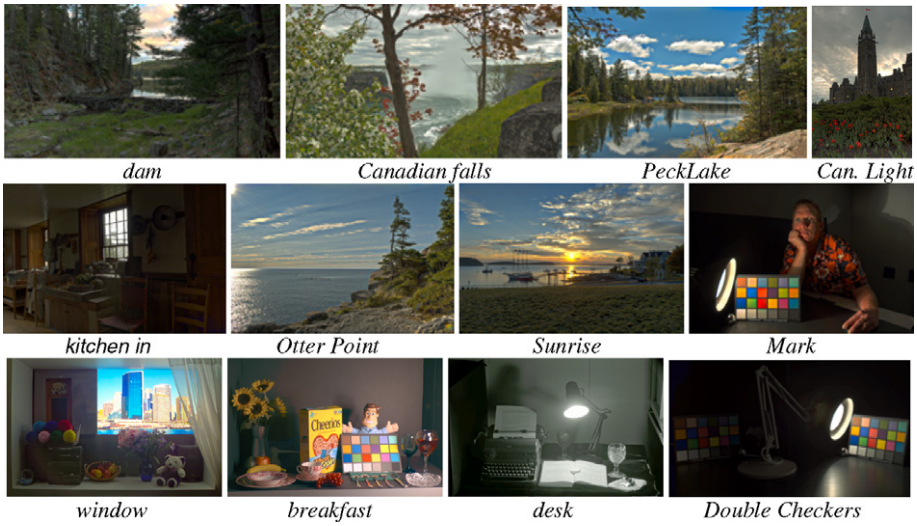

Fig. 6. Thumbnails of experimental images (scenes).

has good homogeneous performance in all test images, mostly in the top group of algorithms. Comparing to iCAM, which performs not as well as most other algorithms for most test images, iCAM06 have been significantly improved. Other algorithms do not exhibit such homogeneity over all the test images as that of iCAM06.

3.4. Results for evaluation of accuracy using real-world scenes

Fig. 10 shows the average overall accuracy scores for four test scenes. These results indicate how well the algorithms reproduce the appearance of the corresponding physical scenes. The overall results show that iCAM06 is ranked first, but not significantly better than the other two Photoshop methods. This group of algorithms has significant better performance than other algorithms.

The results for individual scenes, which are shown in Figs. 11 and 12, provide more insights into the rendering accuracy performance. The test algorithms are grouped into three: iCAM06 and two Photoshop methods have all positive scores over the test images, photographic reproduction and histogram adjustment have all negative scores, and bilateral filter and iCAM do not have the same homogeneity as other algorithms. In the first group, iCAM06 is ranked first in three of the test scenes, performing better or significantly better than the Photoshop local adaptation and exposure and gamma methods. For the scene *window*, Photoshop local adaptation has a much higher accuracy score than iCAM06, which accounts for the approximate balance in the average scores.

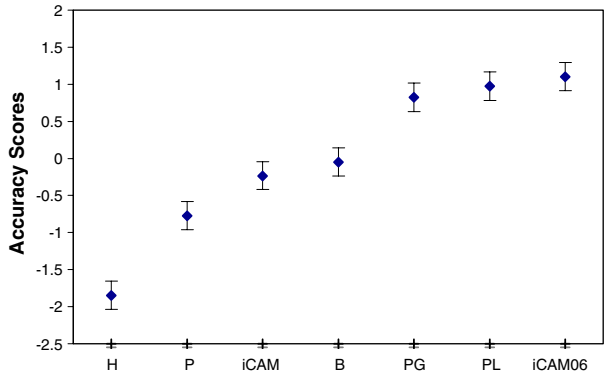

Fig. 10. Overall accuracy scores of tone-mapping operators for 4 real-world scenes.

4. Conclusion

A new image appearance model, iCAM06, has been presented in this paper, which extends the previous model, iCAM, to a large luminance levels ranging from low scotopic to high luminance photopic levels. This model incorpo-

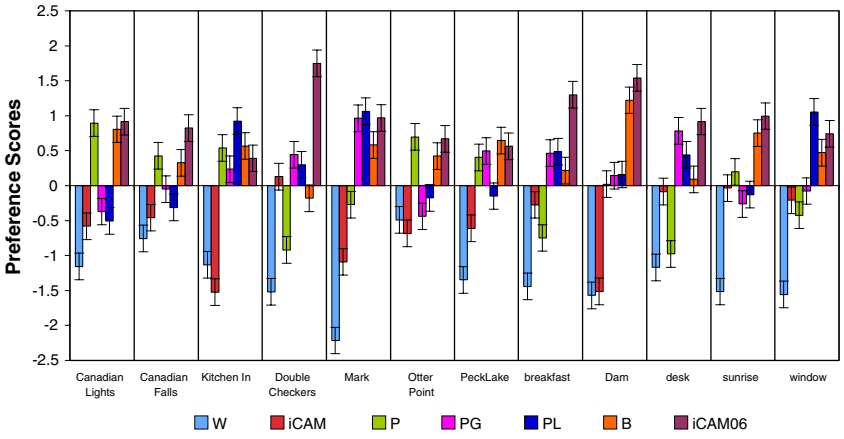

Fig. 8. Preference scores for 12 test images by image.

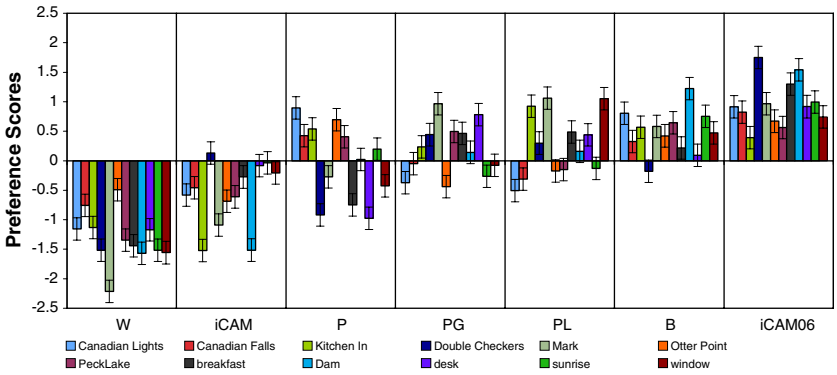

Fig. 9. Preference scores for 12 test images by algorithm.

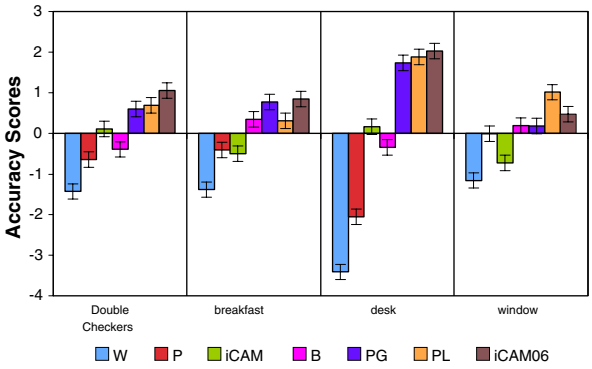

Fig. 11. Accuracy scores for 4 test HDR scenes by scene.

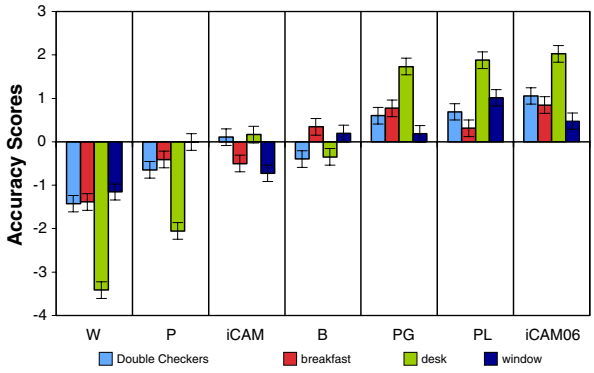

Fig. 12. Accuracy scores for 4 test HDR scenes by algorithm.

rates edge-preserving spatial filtering with human vision photoreceptor response functions in a dual-processing framework. The goal of the new model is to predict image attributes for complex scenes, producing images that closely resemble the viewer's perception when standing in the real environment.

The HDR image rendering performance of iCAM06 was tested in a psychophysical experimental framework using a large variety of test images. The preference results show that iCAM06 has been significantly improved from iCAM and performed significantly better than other test algorithms, including the previous best operator, bilateral filter. The accuracy performance was evaluated by comparisons of rendered images with four real-world scenes. The iCAM06 model was ranked first among all test operators. Although iCAM06 had close accuracy scores with those manual adjustment methods from Photoshop, it significantly outperformed other tone-mapping operators. The consistency of good performance in both preference and accuracy makes iCAM06 a good candidate for a general-purpose tone-mapping operator. The experimental results and Matlab codes of the iCAM06 model are publicly available at http://www.cis.rit.edu/mcsl/icam06/.

References

[1] X. Zhang, B.A. Wandell, A spatial extension to CIELAB for digital color image reproduction, in: Proceedings of the SID Symposiums, vol. 27, 1996, pp. 731–734.
[2] S.N. Pattanaik, J.A. Ferwerda, M.D. Fairchild, D.P. Greenberg, A multiscale model of adaptation and spatial vision for realistic image display, in: Proceedings of ACM-SIGGRAPH, 1998, pp. 287–298.
[3] M.D. Fairchild, G.M. Johnson, Meet iCAM: a next-generation color appearance model, IS& T/SID 10th Color Imaging Conference (2002) 33–38.
[4] M.D Fairchild. G.M. Johnson, Image appearance modeling, in: Proc. SPIE/IS& T Electronic Imaging Conference, SPIE, vol. 5007, 2003, pp. 149–160.
[5] M.D. Fairchild, G.M. Johnson, The iCAM framework for image appearance, image differences, and image quality, J. Electron. Imaging 13 (2004) 126–138.
[6] G.M. Johnson, M.D. Fairchild, Rendering HDR images, IS& T/SID 11th Color Imaging Conference, Scottsdale (2003) 36–41.
[7] J. Kuang, H. Yamaguchi, C. Liu, G.M. Johnson, M.D. Fairchild, Evaluating HDR rendering algorithms, ACM Trans. Appl. Percept. (2007).
[8] F. Durand, J. Dorsey, Fast bilateral filtering for the display of high-dynamic-range image, in: Proceedings of ACM SIGGRAPH 2002, Computer Graphics Proceedings, Annual Conference Proceedings, 2002, pp. 257–266.
[9] J. Kuang, G.M. Johnson, M.D. Fairchild, iCAM for High-Dynamic-Range Image Rendering, in: Proceedings of the 3rd symposium on Applied perception in graphics and visualization APGV '06, 2006.
[10] J. Kuang, High-Dynamic-Range Digital Photography: Image Display and Perception. Ph.D. Thesis, Rochester Institute of Technology. Rochester, 2006.
[11] J. Kuang, M.D. Fairchild, iCAM06, HDR, and Image Appearance, IS& T/SID 15th Color Imaging Conference, Albuquerque, New Mexico, 2007.
[12] IEC 61966-2-1 (1999-10), Multimedia systems and equipment - Colour measurement and management—Part 2-1: Colour management—Default RGB colour space—sRGB, International Electrotechnical Commission, www.srgb.com, 1999.
[13] N. Moroney, M.D. Fairchild, R.W.G. Hunt, C.J. Li, M.R. Luo, T. Newman, the CIECAM02 Color Appearance Model, IS& T/SID 10th Color Imaging Conference, Scottsdale (2002) 23–27.
[14] H. Yamaguchi, M.D. Fairchild, A study of simultaneous lightness perception for stimuli with multiple illumination levels, 12th Color Imaging Conference (2004) 22–28.
[15] F. Ebner, M.D. Fairchild, Development and testing of a color space (IPT) with improved hue uniformity, IS& T/SID 6th Color Imaging Conference, Scottsdale (1998) 9–13.
[16] L. Michaelis, M.L. Menten, Die Kinetik der Invertinwerkung, Bochemische Zeitschrift (1913) 49.
[17] J.M. Valeton, D. van Norren, Light adaptation of primate cones: an analysis based on extracellular data, Vision Res. 23 (1983) 1539–1547.
[18] R.W.G. Hunt, C.J. Li, M.R. Luo, Dynamic cone response functions for models of color appearance, Color Res. Appl. (2003) 79–80.
[19] R.W.G. Hunt, The reproduction of colour, 5th ed., Fountain Press Ltd., 1995.
[20] E. Reinhard, M. Stark, P. Shirley, J. Ferwerda, Photographic tone reproduction for digital images, in Proceedings of ACM SIGGRAPH 2002, Computer Graphics Proceedings, Annual Conference Proceedings, 2002, pp. 267–276.
[21] G.W. Larson, H. Rushmeier, C. Piatko, A visibility matching tone reproduction operator for high dynamic range scenes, IEEE Trans. Vis. Comput. Graph. (1997) 291–306.